Quantitative analysis of the collective behavior in a micromagnetic model

J. M. González
Instituto de Ciencia de Materiales, Consejo Superior de Investigaciones Científicas, Cantoblanco, 28049, Madrid, Spain

O. A. Chubykalo and J. González
Departamento de Física de Materiales, Facultad de Química, Universidad del País Vasco, P. Manuel de Lardizabal, 3, 20080 San Sebastian, Spain

(Received 7 May 1996)

The basic features of the collective demagnetization processes (avalanches) taking place in magnetically ordered systems are investigated in terms of a micromagnetic model of a textured polycrystalline material. The model, considering anisotropy, exchange and Zeeman as well as magnetostatic contributions to the internal energy of the system, is characterized by the possibility of the simultaneous nucleation of different avalanches (at different regions of the system) and by the occurrence of time-dependent effects (associated with thermally activated demagnetization). We have considered a cyclically driven system in which we have quantified the probability $p(L)$ of nucleation of an avalanche of size L (given by the number of grains which reverse their magnetization through such an avalanche). That probability depends on the time for which the system is allowed to relax at every field value, on the total size of the system, and on the model parameters measuring the intrinsic properties of the material. Depending on the ratio, r of a typical structural length (the grain size, measured in number of moments per grain) to the correlation length characterizing the magnetic moment structure, we were able of detect subcritical ($r \gg 1$), supercritical ($r \ll 1$), and critical ($r \simeq 1$) demagnetization regimes. When the system is tuned (for instance, by varying its grain size) to the critical state, the size distribution of the avalanches is characterized by the occurrence of scale invariance with respect to the total size of the system. We have also investigated the statistics of the demagnetization process developing when the system is kept under a constant demagnetizing field. In this particular case and in addition to $p(L)$, we obtained the function $p(T)$ giving the probability of nucleation of an avalanche which propagates during a time T. Our results evidenced the presence of very long tails (of the logarithmic type) in both the $p(L)$ and the $p(T)$ distributions, which were clearly correlated to the logarithmic relaxation of the total magnetization of the system. [S0163-1829(97)01302-7]

I. INTRODUCTION

The occurrence of remanence-type states and that of the associated coercivities are, from the standpoint of their use in practical devices, the more relevant characteristics of the magnetically ordered materials.[1] Although related to the values taken by some intrinsic properties (as the saturation magnetization, the anisotropy, and the exchange interactions) both remanence and coercivity depend on[2] a wide variety of extrinsic features: (i) the crystalochemical properties of the sample, (ii) its macroscopic and microscopic morphology, and (iii) the distribution of defects.[3–5]

There are several difficulties in the modelization of magnetization-reversal processes. First, the concrete distribution of extrinsic characteristics influencing the coercive force value is, generally, very difficult to know in detail. This is due both to the lack of experimental probes allowing one to measure the local anisotropy and/or exchange constants and to the wide range of morphological characteristics that should be considered in order to account for the local demagnetizing effects. A second, and even more relevant, difficulty is related to the presence of both short-range (exchange) and long-range (magnetostatic) interactions which can originate the occurrence of collective demagnetization phenomena.[6]

Considering now this last point, it has been proposed[7–9] that the collective aspects of the demagnetization processes could be discussed in the framework of self-organized criticality (SOC), a concept first introduced by Bak, Tang, and Wiesefeld, widely analyzed in terms of cellular-automaton-like models[10,11] and already brought to a range of phenomena going from martensitic transformations[12] and earthquakes[13] to water droplets[14] and magnetic domain dynamics.[8,9]

From the phenomenological point of view the occurrence of SOC in a given dissipative system requires a large number of metastable states. A slowly driven system possessing that property can evolve through successive transitions between these metastable states to reach a minimally stable one which constitutes an attractor for its dynamics.[15] At that critical state the system reacts to any perturbation through a sequence of collective events (named avalanches) having a finite probability of (i) involving any fraction of the total number of degrees of freedom of the system and of (ii) propagating during any time interval.[10,16,17] By analogy with the phase transitions in finite-size systems (a phenomenology which is linked to the lack of any characteristic time or spatial scale) it has been suggested that the probability distributions of avalanche sizes and lifetimes should obey finite-size scaling relationships. Let us remember too that, differently from the regular critical behavior taking place at phase transitions, SOC occurs spontaneously, that is, without the need of tuning any of the system parameters.

In principle, magnetically ordered systems, and as a con-

sequence of the fact that they possess a huge number of degrees of freedom, meet the basic requirements to exhibit SOC. To make this point clear, let us remember that there are a number of experimental pieces of evidence[18] about the fact that the coherent rotation mechanism does not adequately describe demagnetization processes; i.e., the different degrees of freedom of the magnetic systems do not couple into a few ones during magnetization reversal. Therefore, during demagnetization the systems evolve in a very corrugated energy landscape with many local minima (the relevance of the description in these terms of even the simpler magnetic systems has been recently discussed in the context of the magnetic relaxation phenomenology[19]). The elemental processes involved in the transition between those minima are the nucleation and propagation of domain-wall-like structures.[20]

To summarize the conclusions of the studies linking demagnetization and SOC we can reference (i) the works focusing on the so-called Barkhausen noise,[21–23] which have evidenced that the voltage induced in a pickup coil surrounding a soft sample submitted to a slowly cycled magnetic field exhibits self-similarity over two orders of magnitude in time, (ii) the random bond Ising models,[24] where upon changing the amount of disorder present in the system a phase transition from a subcritical state to a supercritical one occurred (the state defining the transition was characterized by the occurrence of avalanches of all the possible sizes up to that of the system), and (iii) the phenomenological model proposed by Bak and Flyvbjerg for the field-induced reorganization of magnetic domain patterns in perpendicular anisotropy films[8] which shows a subcritical self-organized state.

Nevertheless, the question of the actual occurrence of SOC in magnetic systems is, to our opinion, still open. To make this point clear it is necessary to consider in detail the differences between the cellular automaton models (sandpile models) clearly exhibiting SOC and the realistic models of magnetic systems. A first difference is related to the way in which avalanches are triggered: In the case of the sandpile models a certain part of the system is perturbed and this perturbation can (or not) result in a propagating avalanche. The sandpile models are in most cases very slowly driven which means that once nucleated an avalanche is followed (without any further nucleation) until the system becomes stable again. In contrast with this in an experiment there is not any restriction to the simultaneous triggering and propagation of several collective demagnetizing processes taking place in different regions of the sample. This is due, fundamentally, to the fact that the whole system is under the action of the perturbating agent, i.e., the applied magnetic field. The simultaneous occurrence of avalanches nucleated at different points of the sample leads to the possibility of avalanche coalescence. A second difference is related to the fact that in sandpile models a given avalanche links two essentially equivalent states. Differently from this, the demagnetization avalanches link the remanent (metastable) states with the fully reversed one which, for an applied demagnetizing field, constitutes the absolute energy minimum. Regarding this, it is important to remark that whereas the sandpile models are essentially transport models, demagnetization models should not be included in this category. Thus, a technique globally detecting the collective demagnetization processes cannot, in general, distinguish between a single large avalanche and several simultaneous small ones. From this, it becomes quite evident that a comparison between the predictions of a cellular-automaton-like model and the experimental results presented in Ref. 22 seems not to be appropriate. It is also interesting to recall that the critical behavior found in the random bond Ising models should not be considered as self-organized since the observation of criticality (wide probability distributions of avalanche sizes, and lifetimes) requires in those models the tuning of the degree of the disorder present in the system. To summarize our point, and to the best of our knowledge, there is no nonphenomenological model discussing SOC in magnetic systems and allowing the occurrence of avalanche coalescence (an experimental discussion on coalescing propagating water droplets avalanches is presented in Ref. 14, whereas Ref. 25 gives a theoretical report which thoroughly analyzes coalescing avalanches in sandpile models driven at different rates).

Our aim in the present work is to analyze in terms of a micromagnetic model the collective demagnetization behavior of sets of exchange and magnetostatically coupled units (grains), each one of them having internal structure. In our model the whole system is under the action of an applied field (which is cyclically varied) and its evolution is followed by means of a Monte Carlo algorithm. From the evolution of the system under the action of the field we will evaluate the variation of the probability distributions of avalanche sizes and lifetimes as a function of the size of the system and the parameters giving the intensity of the intergrain coupling. The examination of those distributions will allow us to conclude about the occurrence of critical demagnetization. Also, and since our model allows thermal activation,[19] we will examine the time evolution of the collective demagnetization under constant (nonzero) demagnetizing fields.

II. DESCRIPTION OF THE MODEL

Our simulations have been carried out in the framework of the micromagnetic approximation,[26] a family of models which are widely used to study the phenomenology of magnetic hysteresis in quite realistic terms. Although not strictly realistic (the degree of details of the microstructure description is limited by the available computing power), these models allow one to explore the basic hysteretic properties of permanent magnet materials. The concrete model we used was proposed in Refs. 27 and 28 and sucessfully exploited in the study of thermally activated demagnetization processes.[19,29,30] The modeled system consisted of a long chain of parallel planes, each one representing an atomic plane. Intraplane and interplane exchange constants were considered infinite and finite, respectively, which rendered the model one dimensional (1D), although the individual magnetic moments representing each plane were allowed to orient in 3D. The geometry of the model and the considered reference system are illustrated in Fig. 1. The chain of N planes (each one of them can be represented by a single magnetic moment due to the infinite intraplane exchange) is organized in grains, each one having N_1 planes (magnetic moments) and a particular easy-axis orientation. Thus, the grain boundaries are defined by discontinuities in the local easy axis orientation. The total energy of the system per unit area of the infinite planes, measured in interplanar distance

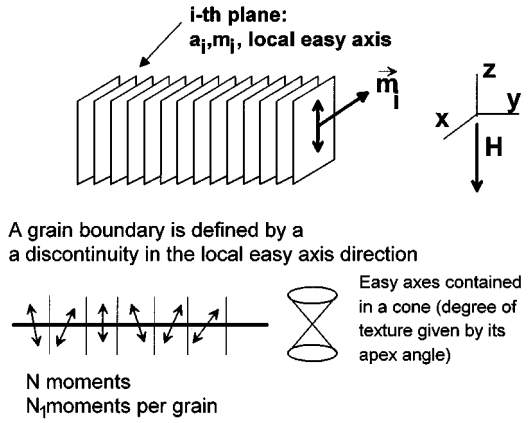

FIG. 1. Sketch of the geometry of the model and reference system used.

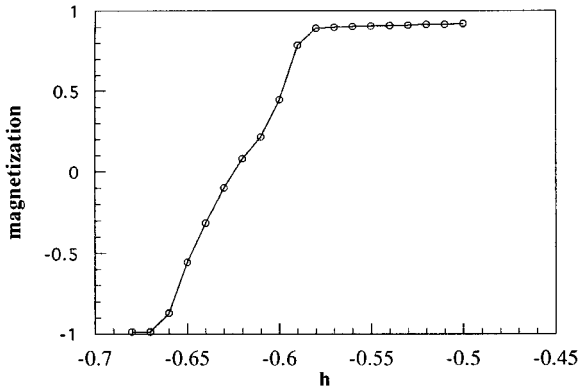

FIG. 2. An example of the demagnetization branch of a hysteresis loop of our system. The parameters of the simulation are $N_1=3$, $N=120$, $a=2$, $m=0.3$, $\Delta h=0.01$ and $\Delta\mathrm{MCS}=500$.

units and normalized to the maximum anisotropy energy, can be given in spherical coordinates as

$$E=\frac{1}{2}\sum_{i=1}^{N}\sin^2\alpha_i-h\sum_{i=1}^{N}\cos(\pi-\theta_i)-a\sum_{i=1}^{N-1}\cos\beta_{i,i+1}+\frac{m}{2}\sum_{i=1}^{N}\sin^2\theta_i\sin^2\phi_i, \quad (1)$$

where θ_i and ϕ_i are the polar and azimuthal angles, corresponding to the ith moment. The first term in Eq. (1) describes the anisotropy energy which we will consider as uniaxial. Here α_i stands for the angle between the direction of the ith magnetic moment and the direction of the corresponding local easy axis. The second term is the Zeeman energy (magnetic field applied along the $-OZ$ direction) which is unidirectional and proportional to coefficient h which gives the applied field in units of the anisotropy field. The third term is an exchange energy whose magnitude is given by coefficient a, the exchange-to-anisotropy energy ratio, and where we take into account only first-neighbor interactions. In this third term, $\beta_{i,i+1}$ denotes the angle between the moments at the ith and $(i+1)$th sites:

$$\cos\beta_{i,i+1}=\cos\theta_i\cos\theta_{i+1}+\sin\theta_i\sin\theta_{i+1}\cos(\phi_i-\phi_{i+1}). \quad (2)$$

Finally, the last term in Eq. (1) represents the magnetostatic energy.[29] Although this term corresponds in general to a many-body interaction, in the 1D case it can be reduced to a local form. The magnitude of the magnetostatic energy is measured by coefficient m, the square of the magnetization-to-anisotropy ratio.

In all the particular systems we have studied we considered textured sets of grains, with Gaussian distributions of easy axes, centered along the OZ axis (see Fig. 1) and having a polar width of 20°. The considered values of the parameters measuring the exchange and magnetostatic couplings corresponded to highly anisotropic materials (we have considered a constant value of the anisotropy constant and therefore variations of the a and m parameters were linked to variations of the exchange constant and of the magnetization, respectively). The hysteretic behavior of the different systems was followed by using a Monte Carlo algorithm with Metropolis dynamics in a canonical ensemble (at a constant temperature corresponding to 10^{-4} of the maximum anisotropy energy attainable by the system).

III. AVALANCHES IN CYCLICALLY DRIVEN SYSTEMS

The simulation of the demagnetization process was carried out considering free boundary conditions at both ends of the system. Starting point of the simulation corresponded to all the magnetic moments pointing parallel to their local easy axes, having positive projections along the OZ axis and under an applied demagnetizing (negative projection along the OZ axis) field value. At this field value the system was allowed to relax during a given number of Monte Carlo steps [a Monte Carlo step (MCS) is defined as the process corresponding to the consecutive introduction of random modifications in the coordinates describing all degrees of freedom of the system]. After this relaxation stage the demagnetizing field was increased by Δh and the system was allowed to relax again for the same number of MCS. The random modifications of the orientation of the magnetic moments used as elemental mechanism for the accomplishment of the relaxation were introduced by changing their polar and azimuthal angles in $\pm 2.5°$. This arbitrary choice resulted in a percentage of moves accepted by the Monte Carlo algorithm of the order of 50%. After this the demagnetization field was incremented and the relaxation procedure repeated until all the grains of the system became in the ''magnetization-reversed state'' (see Fig. 2 for an example of a hysteresis cycle). For the ith grain, the magnetization-reversed state was defined as that corresponding to a negative magnetization value $M_i=\Sigma m_i/N_1$ (where m_i are the components along the OZ axis of all the magnetic moments in the ith grain), verifying $M_i<-\cos^{-1}(\theta_m+\pi/4)$. This condition is based on the orientation of an isolated moment (having exclusively anisotropy and Zeeman contributions to its internal energy), initially oriented along its easy axis (forming an angle of θ_m degrees with the OZ axis), and which, due to the increase of the magnitude of a demagnetizing field pointing along $-OZ$, undergoes an irreversible rotation towards the field direction.

Finally, and for statistical purposes, ensemble averages over a large number of equivalent systems (typically 2000 and in some cases up to 5000) with different easy axis configurations were performed.

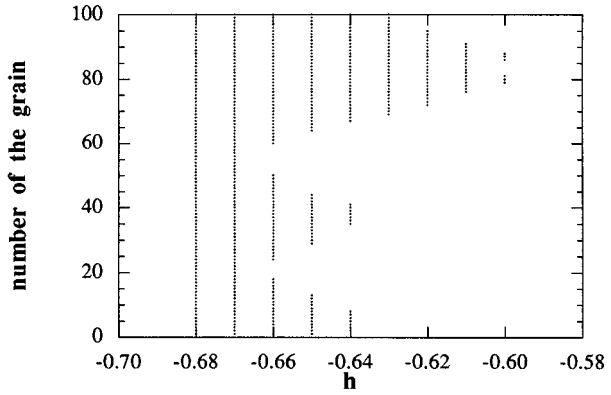

FIG. 3. Schematic representation of the field-evolution of the magnetization of a field cycled system. The dots show the grains in the magnetization-reversed state. The parameters of the simulation are $N_1=3$, $N=300$, $a=2$, $m=0.3$, $\Delta h=0.01$, and $\Delta\mathrm{MCS}=500$.

A. Rule for the evaluation of the avalanche size

Direct examination of the magnetic moment configuration of our system during the development of demagnetization reveals that reversal takes place through the following sequence: (i) rotation towards the field direction of the magnetic moments inside a given grain (a ''rapid'' process, taking typically place in some tens of MCS) and (ii) propagation of the 180° domain-wall-like structures separating a pair of reversed-unreversed grains (a much slower process, developing during MCS, ranges going from several hundreds up to several thousands of MCS). We will identify the latter demagnetization process, being of collective nature, with the occurrence of avalanches. To illustrate graphically the propagation of those avalanches, we will mark with a solid circle (see Fig. 3) all the grains in our system which have reversed their magnetization (in the previously discussed sense) after the relaxation stage corresponding to a given field value. The evolution of these marks with the successive fields gives an idea of the size and localization in the system of the propagating avalanches.

In Fig. 3 it is clearly seen that unlike most models of sandpiles, we have the possibility of avalanche nucleation in different points of our micromagnetic system. The coexistence of the propagation stage of several avalanches nucleated at slightly different fields is possible too. Thus, we should consider two different regimes in the evolution of the system: an initial one (taking place at small field values) corresponding to demagnetization through nonoverlapping avalanches and a second one where avalanches coalesce. Having this in mind, we will introduce the following rule to evaluate the sizes of the avalanches: If a pair of simultaneously nucleated domain walls propagate during several relaxation stages (corresponding to different consecutive field values), we will consider that the size of the associated avalanche coincides with the number of grains swept by the walls until the reversed region gets stable (the next relaxation stage does not lead to the reversal of the grains limiting the reversed region) or it coalesces with a previously reversed (or simultaneously reversing) set of grains. The rule introduces some rounding off errors (linked to the fact that the grains have internal structure) but during our study it has proved to be simple and useful to quantify the avalanche sizes. We should also point out that the avalanches of the size of the system have not been taken into consideration due to the fact that we are not able to discern by only observing its complete reversal if this occurred through a single avalanche or if the reversal proceeded by a sequence of small ones.

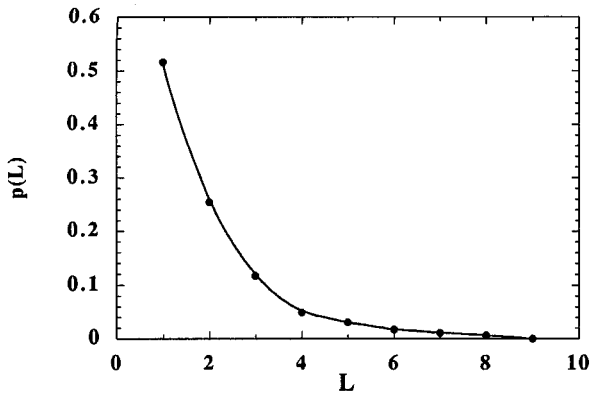

FIG. 4. Distribution of avalaches sizes for ''short'' relaxation stage. The parameters of the simulation are $N_1=10$, $N=600$, $a=2.0$, $m=0.3$, $\Delta h=0.01$, and $\Delta\mathrm{MCS}=200$.

B. Probability distributions of avalanche sizes and the basic characteristics of its dependence on the model parameters

The basic purpose of our study is the investigation of the probability $p(L)$ corresponding to the occurrence of avalanches of a given size L (measured in the number of reversed grains). That probability will, in principle, be related (i) to the rate at which the system is cyclically driven (that is, to the combination of the size of the demagnetizing field increment Δh and of the duration, measured in MCS, of the relaxation stage, Δ MCS), (ii) to the total size of the system, S(measured in number of grains), and (iii) to the particular set of model parameters describing the intergrain interaction.

In order to illustrate the first mentioned dependence we present in Figs. 4 and 5 results corresponding to the probability distributions of avalanche sizes evaluated in systems which were driven at the same Δh and different Δ MCS values. Data in Fig. 4 correspond to a system for which a relaxation stage with duration $\Delta\mathrm{MCS}=200$ was allowed. As

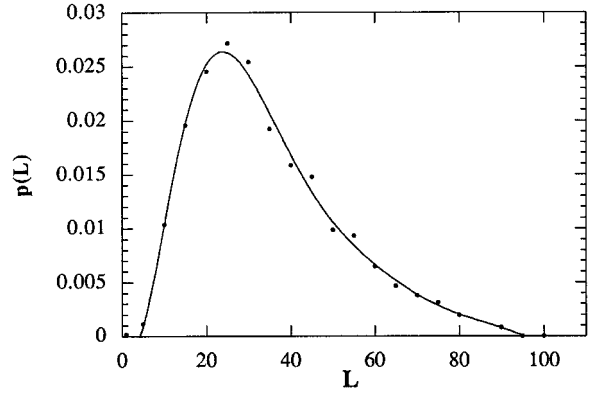

FIG. 5. Distribution of avalanche sizes for the ''long'' relaxation stage. The parameters of the system are $N_1=10$, $N=1000$, $a=2.0$, $m=0.3$, $\Delta h=0.01$, and $\Delta\mathrm{MCS}=4000$.

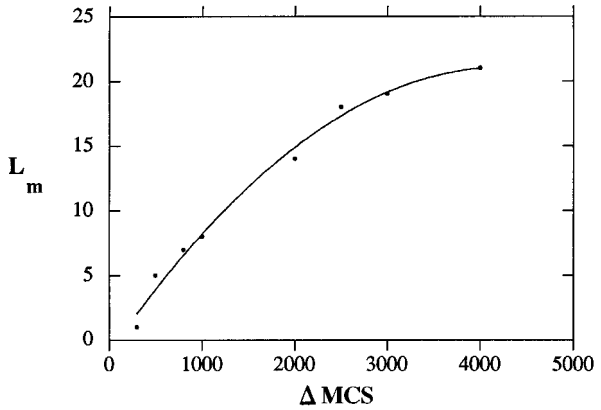

FIG. 6. Size of the most probable avalanche vs the number of Monte Carlo steps. The parameters of the simulation are $N_1=10$, $N=4000$, $a=1.0$, $m=0.3$, and $\Delta h=0.01$.

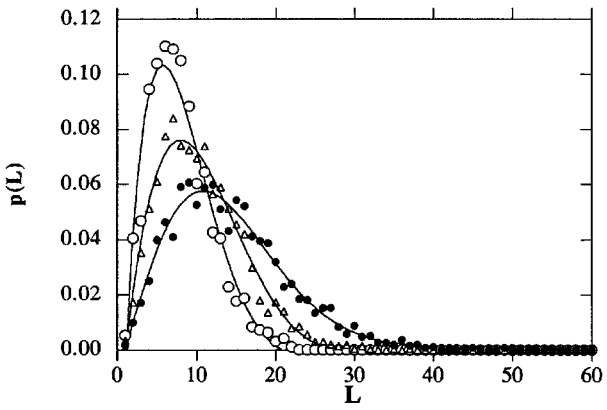

FIG. 7. Distribution of avalanche sizes for different values of the exchange parameter a:(○)$a=1.5$, (△)$a=2.5$, and (●)$a=5.0$. The parameters of the simulation are $N_1=10$, $N=800$, $m=0.3$, $\Delta h=0.01$, $\Delta\mathrm{MCS}=500$.

is clear from the figure under these particular conditions the probability of observing an avalanche of a given size decreases monotonically with an increase of the size of the avalanche and small size avalanches are mostly observed. In the case of a longer relaxation stage (see Fig. 5) the probability distribution shows a maximum at a size L_m and spans for a larger avalanche size range (depending on the model parameters that range can go up to the total size of the system). Taking into account these results and in order to obtain nontrivial information about our systems we have chosen the following set of field cycling parameters: $\Delta h=10^{-2}$ and $\Delta\mathrm{MCS}=500$. These values were sufficient to observe, in every studied system and at every field value, several avalanches. Those avalanches led to the magnetization reversal of, at least, 5% of the total number of grains in the considered system. For these relaxation conditions the typical probability distribution of avalanche sizes evaluated in sufficiently large systems has a maximum L_m. In close relation to the previous remarks L_m grows when we increase the duration of the relaxation stage (see Fig. 6).

The most probable avalanche size L_m depends also on the a and m parameters. As far as the a parameter describes the exchange coupling (and, more concretely, the exchange coupling at the grain boundaries) the probability corresponding to the occurrence of the complete reversal of a pair of reversed-unreversed neighboring grains increases with the increase of a. This, in turn, leads to the increase with a of the size of the most probable avalanche (see Fig. 7).

Regarding the influence on $p(L)$ of the m parameter we should point out that the magnetostatic one is, in order of magnitude, the smaller contribution to the system internal energy. It represents, nevertheless, a long-range interaction and its role is crucial in the determination of the particular domain structure present in a given magnetic system and, consequently, in that of many of the characteristics of its hysteretic behavior. From the point of view of the collective behavior, magnetostatic interactions tend to reinforce the intergranular coupling effect of the exchange interactions, thus leading to a shift of the $p(L)$ distribution towards larger avalanche sizes. Due to the large degree of texture of the distribution of local easy axes we considered, the effect of a variation of the magnetization is, in our particular system, weak: According to our results, the variation of the m parameter from 0.1 to 0.35 ($a=2,\Delta h=0.01,\Delta\mathrm{MCS}=500$) is associated with an increase of the L_m value from 7 to 8.

Finally, the dependence of the probability distribution of avalanche sizes on the total size of the system, S, is presented in Fig. 8. A markedly different behavior was observed for small and large system sizes. More concretely, in the case of the smaller systems, the distribution exhibits some structure which we suggest is related to finite-size effects (as the preferred nucleation of avalanches at the two extremes of the system), to the observed reproducibility of the sequence of avalanches (which is linked to the effectiveness as pinning centers of the grain boundaries with a large associated change in the local easy axis direction), and to the rounding errors which are inherent to our avalanche size evaluation rule. As the size of the system increases the distribution becomes smoother and L_m increases with an increase of S, reaching a saturation for sufficiently large systems. This last result is a direct consequence of the possibility of simultaneous nucleation and propagation of avalanches which can later coalesce.

Avalanche overlapping and, again, our avalanche size evaluation rule lead to the invariance, when $S\gg L_m$, of the probability distribution of avalanche sizes with the total size

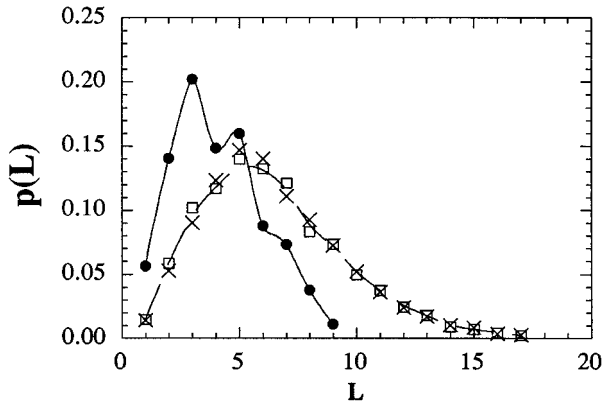

FIG. 8. Distribution of avalanche sizes for the system of small [(●)$S=10$ grains] and large [(□)$S=120$ grains, (×)$S=200$ grains] sizes. The parameters of the simulation are $N_1=10$, $a=1.0$, $m=0.3$, $\Delta h=0.01$, and $\Delta\mathrm{MCS}=500$.

of the system (see Fig. 8). The observation of this invariance effectively reduces, in which concerns the growth of avalanches, the total size of the system to a value which is of the order of the saturation value of the variation of L_m with S.

C. Examination of the occurrence of a critical state

In our search for the possible occurrence of critical demagnetization (always in systems having a maximum total size $S \simeq L_m$) we have taken into account the relationship between the correlation lengths associated with the magnetic interactions and those corresponding to the particular microstructure of our system. Regarding the magnetic correlation lengths we can define those linked to the exchange, l_{ex}, and magnetoelastic, l_{dip}, interactions, as

$$l_{\mathrm{ex}} \propto \sqrt{A/K} \tag{3}$$

and

$$l_{\mathrm{dip}} \propto \sqrt{\mu_0 M_s^2/2K}, \tag{4}$$

respectively. Both correlation lengths give the order of magnitude of the spatial dimensions of a magnetic moment structure which is nucleated from a saturated state in a system in which that nucleation process is essentially ruled by each one of the two interactions. In our particular case and considering the high degree of texture of our model system (let us remember that the easy axis distribution is contained in a cone having an apex angle of 20°) and the consequential fact that, at the remanent states, the magnetic moment distribution will not exhibit large discontinuities in the orientation of the local moments, we do not expect a large influence of the magnetostatic interactions on the demagnetization process. The weak influence of those interactions on the nucleation process was confirmed by a recent study of the coercitivity in the same model system[30] which evidenced the fact that the coercive force of the system changed only in 10^{-2} of the anisotropy field when the magnetization was increased in a 50% field. Therefore, the correlation length relevant to describe the demagnetization of our system will be l_{ex}. To give a concrete expression for this correlation length we have taken into consideration the typical inhomogeneities present in the magnetic moment configuration prior to the onset of the reversal process, those present at the grain boundaries and associated with the transition between two differently oriented local easy axes. An estimation for the typical width of such domain-wall-like structures is

$$l_{ex} = \theta_m \sqrt{A/K} = \theta_m \sqrt{a}. \tag{5}$$

Taking this into account we define a coefficient r giving the ratio of the most characteristic structural length, the grain size N_1, to l_{ex} as

$$r = N_1 / \theta_m \sqrt{a}. \tag{6}$$

Next, we will examine the statistics of the collective demagnetization for (i) $r \gg 1$, (ii) $r \ll 1$, and (iii) $r \simeq 1$. Besides this, for a given set of parameters, we should limit ourselves to systems sizes of the order of the most probable avalanche size in order not to have too many coalescing events and to obtain a behavior as close as possible to that of a slowly driven system. The concrete region of model parameters we explored was defined by $2 < N_1 < 10$, $1 < a < 20$, and $0.10 < m < 0.35$.

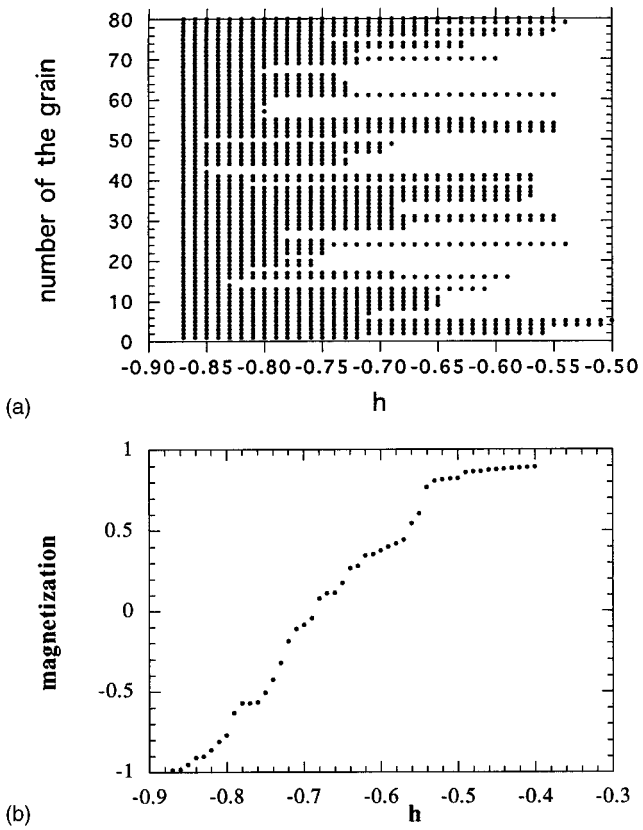

FIG. 9. (a) Schematic representation of the avalanches in the subcritical state. The parameters of the simulation are $N_1 = 3$, $N = 240$, $a = 0.1$, $m = 0.3$, $\Delta h = 0.01$, and $\Delta \mathrm{MCS} = 500$. (b) Demagnetization branch corresponding to the avalanches of (a).

If $r \gg 1$, the thickness of the propagating domain wall [given by $\pi l_{\mathrm{ex}} / \theta_m$ (Ref. 31)] is smaller than the size of an individual grain (it is, in fact, of the order of the interplanar distance). Also, if we consider always systems having the same N_1 value, the achievement of the $r \gg 1$ condition corresponds to small exchange values. In this case, due to the small intergranular coupling and the large efficiency as pinning centers of the grain boundaries only small size avalanches occur [see Figs. 9(a) and 9(b), where a particular example of the field evolution of the avalanche distribution and the associated demagnetizing branch of the hysteresis loop are shown]. An example of the distribution of avalanche sizes corresponding to this limit is presented in Fig. 10. As is possible to observe there, the distribution of avalanche sizes decreases exponentially and does not depend on the total size of the system. By analogy with the behavior of the cellular automaton models of sandpiles we will consider that the demagnetization in systems characterized by $r \gg 1$ is of the subcritical type.

The opposite limit $r \ll 1$ is characterized by the occurrence of a strong intergranular coupling and large domain wall thicknesses (which are much larger than the grain size). Then, all the grains have a marked tendency to couple during the magnetization reversal in a unique, system-sized avalanche. This behavior is illustrated in Figs. 11(a) and 11(b).

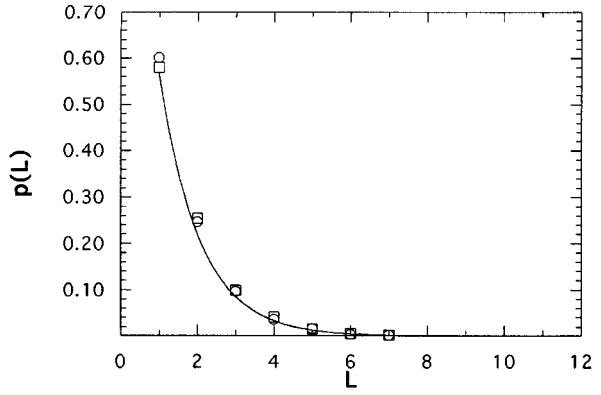

FIG. 10. Distribution of avalanche sizes in the subcritical state. The parameters of the simulation are $N_1=3$, $a=0.1$, $m=0.3$, $\Delta h=0.01$, and $\Delta\mathrm{MCS}=500$. (○)$S=40$ grains and (□)$S=150$ grains.

Of course in this limit the probability distribution function is δ-like, peaking at the system size. Again, and analogously to the behavior of sandpile models, we will consider a system verifying $r\ll 1$ as being supercritical.

When $r\simeq 1$ [see Fig. 12(a)] the distributions of avalanche sizes cover the full possible range from one grain up to the complete size of the system. The demagnetization process seems then to take place in this case through a critical mechanism. It is interesting to point out that, for the different systems verifying the $r\simeq 1$ condition we have considered, L_m is always close to $S/2$. This result is related to the low rate of avalanche nucleation observed under these simulation conditions: We observe, typically, the nucleation of only two avalanches for field cycle. Those avalanches have sizes which are approximately complementary with respect to the total size of the system. The occurrence of criticality when the system is tuned to have similar structural and magnetic correlation lengths is confirmed by the fact that the $p(L)$ distributions exhibit scale invariance [as shown in Fig. 12(b)]. The considered scaling function is of the form

$$p(L)=S^{-\beta}f(L/S^{\nu}). \tag{7}$$

The critical exponents obtained from the scaling process of our simulation data, being both of them close to 1, are clearly related to the $L_m=S/2$ relationship.

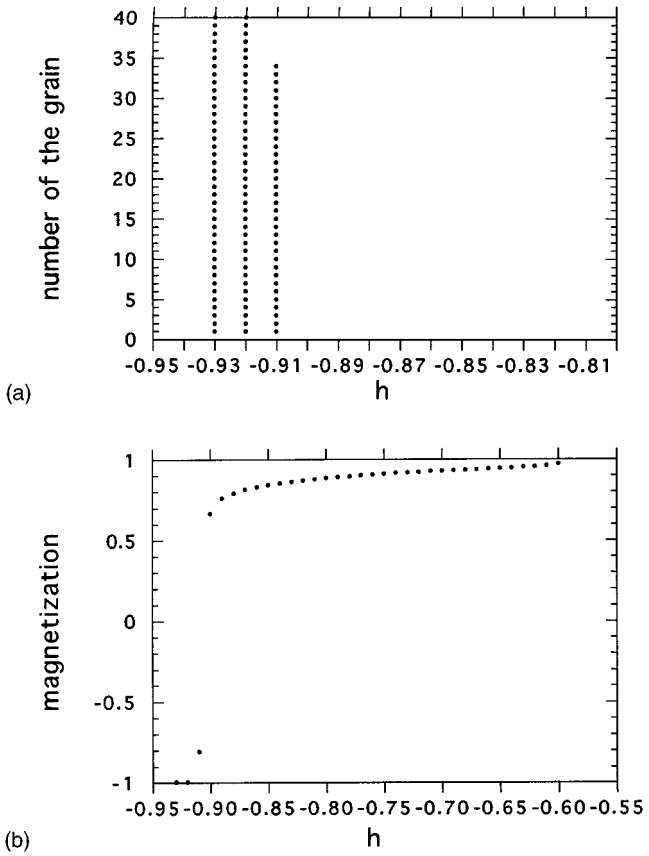

FIG. 11. (c) Schematic representation of avalanches in the supercritical state. The parameters of the simulation are $N_1=3$, $N=120$, $a=100$, $m=0.3$, $\Delta h=0.01$, and $\Delta\mathrm{MCS}=40000$. (b) Demagnetization branch corresponding to the avalanches of (a).

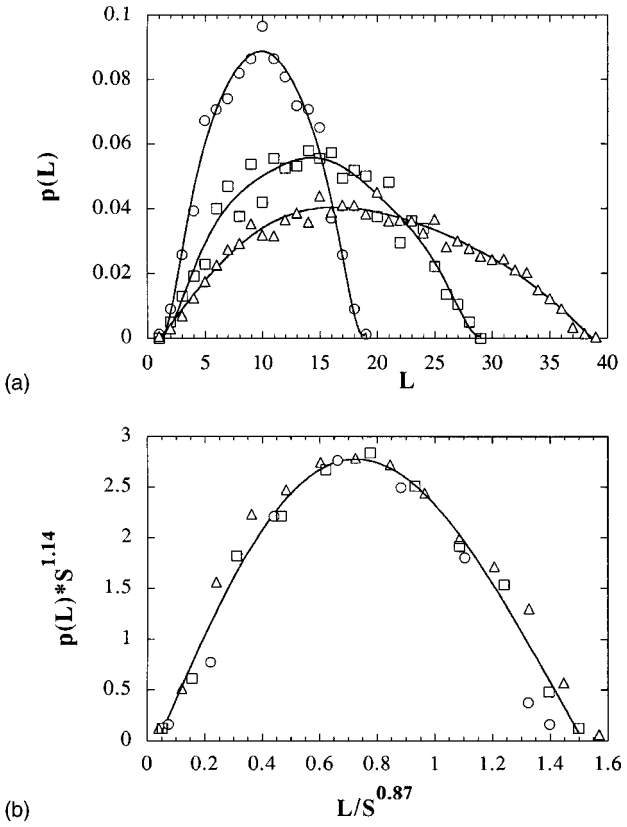

FIG. 12. (a) Distribution of avalanche sizes in the critical state for systems of different sizes: (○)$S=20$ grains, (□)$S=30$ grains, and (△)$S=40$ grains. The parameters of the simulation are $N_1=3$, $a=2.0$, $m=0.3$, $\Delta h=0.01$, and $\Delta\mathrm{MCS}=500$. (b) Scaling of the results in (a).

IV. AVALANCHES IN RELAXATIONAL PROCESSES

Direct examination of the time (MCS) evolution of the configuration of the system when it relaxes under a constant applied demagnetizing field of magnitude similar to that of the coercive force (Fig. 13) reveals the occurrence of ava-

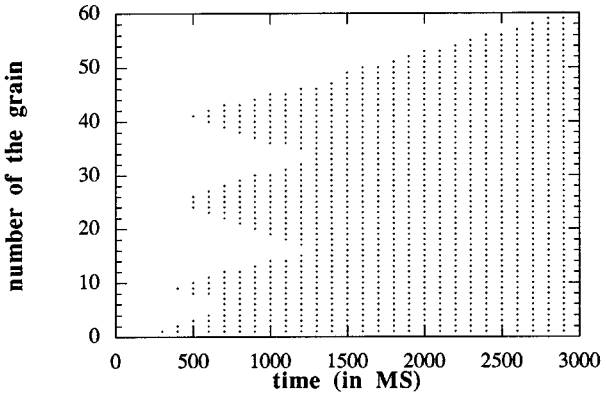

FIG. 13. Schematic representation of avalanches in a relaxing system. The parameters of the simulation are $N_1=3$, $N=180$, $a=2.0$, $m=0.3$, $h=0.7$, and $\Delta\mathrm{MCS}=100$.

lanches and avalanche coalescence (the nucleation of the first avalanches takes always place after a certain waiting time, which evidences the non-Arrhenius relaxation dynamics[19]). We have quantified those collective phenomena by evaluating their size distribution $p(L)$ and their duration distribution $p(T)$ (the probability of observing an avalanche which propagates for a time T). We should point out here that in this relaxational process the time analogous to the discrete field increment we considered in the case of the cyclically driven system is not well defined (an adequate time interval between successive observations of the system should avoid to divide a large avalanche into many small ones or to add up many small uncorrelated demagnetization events). We have arbitrarily chosen $\Delta\mathrm{MCS}=100$.

The $p(L)$ and $p(T)$ distributions corresponding to different values of the external field are shown in Figs. 14(a) and 14(b), respectively. As can be seen in those figures the avalanches occur in lage time intervals and have a broad distribution of sizes with a logarithmiclike tails (see Fig. 15). This fact is in close relation to the time dependence of the total magnetization of similar systems which exhibits a logarithmic decay (Fig. 16). Also in Figs. 14(a) and 14(b), it is possible to observe that when the field is increased the system is less stable at the remanence-type states and therefore the demagnetization avalanches are larger in size and shorter in duration.

Finally, we should remark that the avalanche size and duration distribution functions are system size invariants [see Figs. 17(a) and 17(b)]. To our opinion this fact is linked to the occurrence in our system of different easy axis discontinuities across the grain boundaries which act as multiple centers (with distributed efficiencies) for avalanche nucleation.

V. CONCLUSIONS

We have quantified the collective demagnetization phenomenology occurring in a micromagnetic model of a textured polycrystal which was submitted to a cyclic magnetic field. The basic tool for that was the introduction of a rule allowing us to evaluate the avalanche sizes from previous knowledge of the magnetic moment configuration obtained by relaxing the system at each successive field value. We

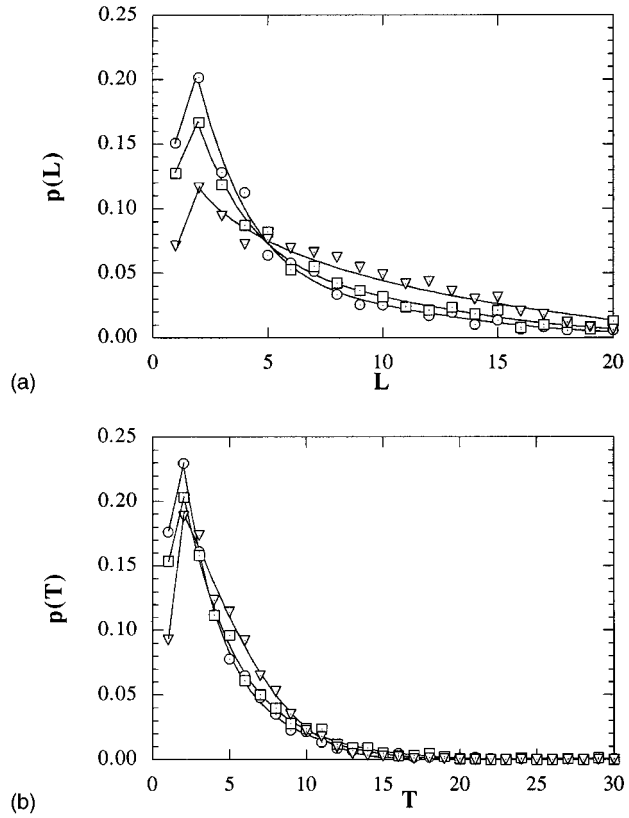

FIG. 14. (a) Distribution of avalanche sizes in a relaxing system for different values of applied demagnetized field [(○)$h=0.68$, (□)$h=0.7$, and (▽)$h=0.74$. The parameters of the simulation are $N_1=3$, $N=180$, $a=2.0$, $m=0.3$, and $\Delta\mathrm{MCS}=100$. (b) The same as in (a) but for the distribution of avalanches durations.

have investigated the influence on the distribution of avalanche sizes of (i) the time the system relaxes at every field value, (ii) the micromagnetic parameters giving the intrinsic properties of the material (such as the exchange parameter a and the magnetostatic constant m), and (iii) the total system size. From the corresponding results we conclude that (i) whereas short-time relaxations exclusively allow the development of small avalanches, larger relaxation stages have associated avalanche sizes distributions exhibiting a most probable avalanche size L_m, which increases with the mag-

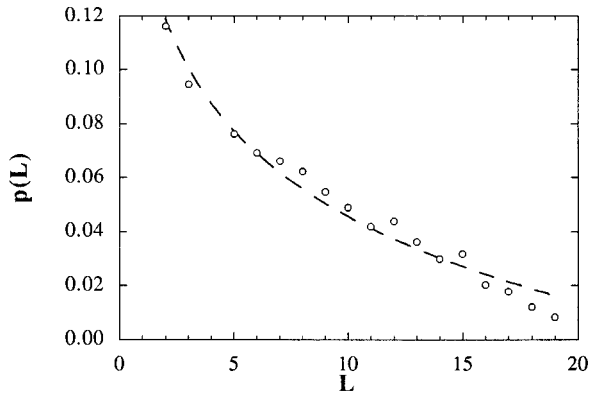

FIG. 15. Logarithmic fit of the curve corresponding to $h=0.74$ in Fig. 14(a).

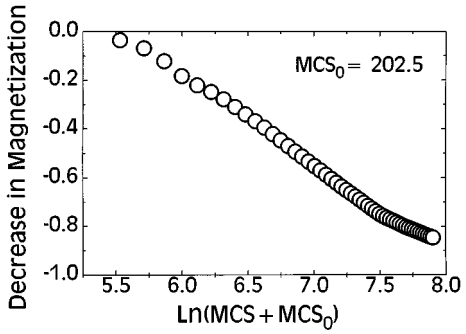

FIG. 16. Time (MCS) dependence of the magnetization plotted as a function of $\ln(\mathrm{MCS}+\mathrm{MCS}_0)$. The parameters of the simulation are: $N_1=50$, $N=104$, $a=2.0$, $m=0.3$, $\Delta h=0.01$, and $\Delta\mathrm{MCS}=500$.

nitude of the relaxation time, the a parameter, and (more weakly) with the m parameter, (ii) the occurrence of avalanche coalescence in sufficiently large systems leads to a saturation of the L_m value, and (iii) the occurrence of avalanche coalescence reduces the effective size of the system in the sense that large size systems (systems having a dimension clearly larger than the typical avalanche size for which avalanches overlap) have identical avalanche size distributions.

From the examination of the distribution of avalanche sizes obtained in systems with $S \simeq L_m$ and having different values of the ratio of the structural-to-magnetic correlation lengths, it was possible to conclude about the occurrence of different collective demagnetization behaviors. When the system parameters, (and basically the exchange parameter) are tuned to a situation in which both correlation lengths are of similar magnitude we detect the occurrence of critical behavior in the sense that the distributions of avalanche sizes span the whole size of the system and are scalable. Since this phenomenology is associated to a limited set of model parameters we cannot consider the critical behavior as self-organized. Large and small values for the above-mentioned ratio between the characteristics lengths of the system lead to subcritical (predominance of small avalanches) and supercritical (predominance of system-sized avalanches) behaviors, respectively.

We have also followed the collective demagnetization during the relaxation of the system at constant applied demagnetizing field. The distributions of avalanche sizes and durations exhibited long logarithmic tails which depended on the applied field value but not on the system size. From this and the clear correlation of the avalanche distribution characteristics to the time dependence of the magnetization we conclude that during relaxation collective demagnetization is linked to the presence of distributed centers of avalanche nucleation.

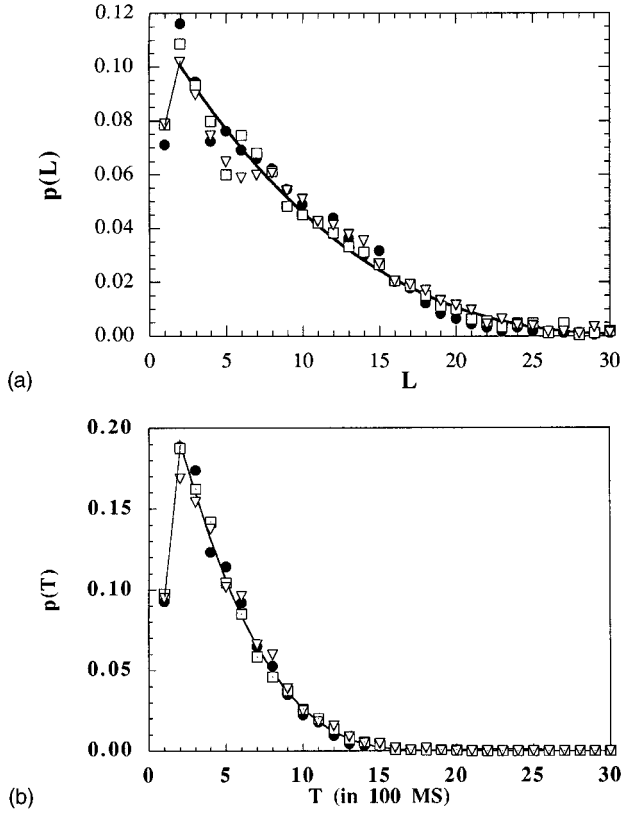

FIG. 17. (a) Distribution of avalanche sizes for a relaxing systems having different system sizes [(●)$S=60$ grains, (□)$S=100$ grains, and (▽)$S=150$ grains]. The parameters of the simulation are $N_1=3$, $a=2.0$, $m=0.3$, $h=0.74$, $\Delta\mathrm{MCS}=100$. Fig. 17(b) The same as in Fig. 17(a) but for the distribution of avalanche durations.

ACKNOWLEDGMENTS

The work was partially suported by Project No. PB93-0123 (Spanish DGICyT). O.A.C. is indebted to the Basque Country Government for financial support. The authors acknowledge useful discussions with K. Kulakowski, R. Ramírez, and R. Smirnov-Rueda.

[1] K.H.J. Buschow, in *Supermagnets, Hard Magnetic Materials*, edited by G.J. Long and F. Grandjean (Kluwer Academic Publishers, Dordrecht, 1990), p. 49.

[2] D. Givord, Q. Lu, and M.F. Rossignol, in *Science and Technology of Nanostructured Magnetic Materials*, edited by G.C. Hadjipanayis and G.A. Prinz (Plenum Press, New York, 1990), p. 635.

[3] G.C. Hadjipanayis, in *Science and Technology of Nanostructured Magnetic Materials*, edited by G.C. Hadjipanayis and G.A. Prinz (Plenum Press, New York, 1990), p. 607.

[4] J. Fidler, Philos. Mag. B **46**, 565 (1982).

[5] H. Kronmüller, K.-D. Durst, and G. Martinek, J. Magn. Magn. Mater. **69**, 149 (1987).

[6] D. Givord, P. Tenaud, and T. Viadieu, J. Magn. Magn. Mater. **72**, 247 (1988).

[7] P. Sethna, K. Dahmen, S. Kartha, J. Krumhansl, B.W. Roberts, and J.D. Shore, Phys. Rev. Lett. **70**, 3347 (1993).

[8] P. Bak and H. Flyvbjerg, Phys. Rev. A **45**, 2192 (1992).

[9] K.L. Babcock and R.M. Westervelt, Phys. Rev. Lett. **64**, 2168 (1990).

[10] P. Bak, C. Tang, and K. Wiesenfeld, Phys. Rev. Lett. **59**, 381 (1987).
[11] L.P. Kadanoff, S.R. Nagel, L. Wu, and S.M. Zhou, Phys. Rev. A **39**, 6524 (1989).
[12] E. Vives, J. Ortin, L. Mañosa, I. Rafols, R. Perez-Magrane, and A. Planes, Phys. Rev. Lett. **72**, 1694 (1994).
[13] Z. Olami, H.J.S. Feder, and K. Christensen, Phys. Rev. Lett. **68**, 1244 (1992).
[14] B. Plourde, F. Nori, and M. Bretz, Phys. Rev. Lett. **71**, 2749 (1993).
[15] S.N. Coppersmith and P.B. Littlewood, Phys. Rev. B **36**, 311 (1987).
[16] T. Hwa and M. Kardar, Phys. Rev. Lett, **62**, 1813 (1989).
[17] H. Flyvbjerg, Phys. Rev. Lett. **76**, 940 (1990).
[18] H. Kronmüller, K.-D. Durst, and M. Sagawa, J. Magn. Magn. Mater. **74**, 291 (1988).
[19] J.M. González, R. Ramírez, R. Smirnov-Rueda, and J. González, Phys. Rev. B **52**, 16034 (1995).
[20] J.M. González and F. Cebollada, Jpn. J. Appl. Phys. **33**, 173 (1994).
[21] O. Geoffroy and J.L. Porteseil, J. Magn. Magn. Mater. **97**, 205 (1991).
[22] O. Geoffroy and J.L. Porteseil, J. Magn. Magn. Mater. **133**, 1 (1994).
[23] P.J. Cote and L.V. Meisel, Phys. Rev. Lett. **67**, 1334 (1991).
[24] E. Vives and A. Planes, Phys. Rev. B **50**, 3839 (1994).
[25] T. Hwa and M. Kadar, Phys. Rev. A **45**, 7002 (1992).
[26] W.F. Brown, Jr., Phys. Rev. **58**, 736 (1940); **60**, 139 (1940).
[27] A. Hernando, I. Navarro and J.M. González, Europhys. Lett. **20**, 175 (1992).
[28] J.M. González, F. Cebollada, and A. Hernando, J. Appl. Phys. **73**, 6943 (1993).
[29] R. Rueda, R. Ramirez, J. González, L. Dominguez, and J.M. González, J. Magn. Magn. Mater. **140-144**, 1843 (1995).
[30] J.M. González, R. Smirnov-Rueda, F. Cebollada, and J. González, IEEE Trans. Magn. (to be published).
[31] S. Chikazumi, *Physics of Magnetism* (Kieger, New York, 1978), p. 186.